Philosophical Magazine, 2015
Vol. 95, No. 23, 2527–2538, http://dx.doi.org/10.1080/14786435.2015.1066041

Martensitic transformation in as-grown and annealed near-stoichiometric epitaxial Ni_2MnGa thin films

P. Machain[a], A.M. Condó[a,b], P. Domenichini[a], G. Pozo López[c,d], M. Sirena[a,b], V.F. Correa[a,b] and N. Haberkorn[a,b]*

[a]*Instituto Balseiro, Universidad Nacional de Cuyo, Av. Bustillo 9500, 8400 San Carlos de Bariloche, Argentina;* [b]*Centro Atómico Bariloche, Comisión Nacional de Energía Atómica, Av. Bustillo 9500, 8400 San Carlos de Bariloche, Argentina;* [c]*Facultad de Matemática, Astronomía y Física, Universidad Nacional de Córdoba, Ciudad Universitaria, 5000 Córdoba, Argentina;* [d]*Instituto de Física Enrique Gaviola – CONICET, Argentina*

(*Received 17 April 2015; accepted 18 June 2015*)

Magnetic shape memory nanostructures have a great potential in the field of the nanoactuators. The relationship between dimensionality, microstructure and magnetism characterizes the materials performance. Here, we study the martensitic transformation in supported and free-standing epitaxial $Ni_{47}Mn_{24}Ga_{29}$ films grown by sputtering on (0 0 1) MgO using a stoichiometric Ni_2MnGa target. The films have a Curie temperature of ~390 K and a martensitic transition temperature of ~120 K. Similar transition temperatures have been observed in films with thicknesses of 1, 3 and 4 μm. Thicker films (with longer deposition time) present a wider martensitic transformation range that can be associated with small gradients in their chemical concentration due to the high vapour pressure of Mn and Ga. The magnetic anisotropy of the films shows a strong change below the martensitic transformation temperature. No features associated with variant reorientation induced by magnetic field have been observed. Annealed films in the presence of a Ni_2MnGa bulk reference change their chemical composition to $Ni_{49}Mn_{26}Ga_{25}$. The change in the chemical composition increases the martensitic transformation temperature, being closer to the stoichiometric compound, and reduces the transformation hysteresis. In addition, sharper transformations are obtained, which indicate that chemical inhomogeneities and defects are removed. Our results indicate that the properties of Ni–Mn–Ga thin films grown by sputtering can be optimized (fixing the chemical concentration and removing crystalline defects) by the annealing process, which is promising for the development of micromagnetic shape memory devices.

Keywords: thin films; martensitic transformations; material preparation

1. Introduction

Low-dimensional systems based in ferromagnetic shape memory Heusler alloys have attracted much attention due to their possible application in microactuators [1–3]. The magnetic shape memory (MSM) effect consists of a magnetic field-induced twin rearrangement within the martensitic phase based on a strong magnetocrystalline anisotropy

*Corresponding author. Email: nhaberk@cab.cnea.gov.ar

[4,5]. The high magnetocrystalline anisotropy and low elastic shear modulus of martensite enable twin boundary displacement in response to the application of a magnetic field. In recent years, great effort has been oriented towards the development of epitaxial Ni–Mn–Ga thin films to obtain the MSM effect [6–8]. Deformation up to 12% has been obtained in free-standing Ni–Mn–Ga thin films by tensile experiments in the martensitic state [9]. MSM also has been observed in micro bridges by applying magnetic field [10]. However, high twinning stress (σ_{tw}) of the $(1\,0\,1)_M$ twin boundary is usually found in thin films [9]. In addition, no large deformation induced by magnetic field (in comparison with single crystals) has been reported [11]. Ni–Mn–Ga single crystals present σ_{tw} of approximately 2 MPa [12], whereas $\sigma_{tw} \approx 25$ MPa has been reported in epitaxial Ni–Mn–Ga films [10]. This fact could be attributed to the complex microstructure that results from the twinned structure, which acts as an obstacle for twin mobility [13]. In fact, MSM effect in Ni–Mn–Ga thin films requires the optimization in the sample growth and the elimination of crystalline defects and disorder that could contribute to an increase of σ_{tw}.

The Ni–Mn–Ga alloy [14] presents a transformation from austenite ($L2_1$) to a combination of modulated martensite (five-layered modulated 5M and seven-layered modulated 7M) and non-modulated (NM) martensite [15,16]. The type of martensitic structure depends on the chemical composition, temperature and applied stress [17,18]. The lattice parameters a_M and c_M of the martensitic phase determine the type of structure. The presence of 5M or 7M structures can be also predicted by the average number of valence electrons per atom (e/a). The critical value is $e/a \approx 7.61$–7.62 [19]. Both 5M (also called 10M) and 7M (also called 14M) structures are interpreted in terms of nanotwin combination of the tetragonal NM martensite, as proposed by the adaptive phase theory [20]. The experimental MSM strain was found to be almost equal to the theoretical maximal value being approximately 6% for 5M phase [21] and 10% for 7M phase [22]. The NM martensite with tetragonal unit cell with $c_M/a_M > 1$ does not show strain by applying a magnetic field [23]. The reason for this is the high twinning stress in the NM phase ($\sigma_{tw} \approx 6$–18 MPa). The easy magnetization axis (magnetocrystalline anisotropy) for the martensite (referred to the high temperature cubic austenite axes) changes from $[0\,0\,1]_A$ to $[1\,1\,0]_A$ when changing from the modulated martensite to the NM martensite [24,25].

In this work, the magnetic properties and the resulting martensitic transformation in near-stoichiometric Ni_2MnGa thin films have been analyzed. Initially, $Ni_{47}Mn_{24}Ga_{29}$ films of different thicknesses (1, 3 and 4 μm) were grown on (0 0 1) MgO substrates, with a Cr buffer layer, by DC magnetron sputtering using a target of Ni_2MnGa. All the films have a martensite start transformation temperature (M_s) of 120 (5) K and a transformation hysteresis around 25 K. We observe broader martensitic transformation for thicker films. No features associated with MSM behaviour were observed by magnetization measurements. In order to verify the possible role of chemical inhomogeneities in the resulting martensitic transformation, the 3-μm film was annealed in the presence of a bulk Ni_2MnGa reference for 20 and 60 min at 1073 K. The film changes the chemical composition from $Ni_{47}Mn_{24}Ga_{29}$ to $Ni_{49}Mn_{26}Ga_{25}$ by the control of the vapour pressure given by the presence of the reference sample. The obtained films show an increment of the M_s and a strong reduction of the hysteresis of the transformation. In addition, a sharper transition is observed for annealed samples, which can be associated with a reduction of chemical gradients and inhomogeneities. All the films (as-grown and

annealed) present an austenitic phase with weak magnetic anisotropy, and a noticeable increment of the magnetic anisotropy in the martensitic phase.

2. Experimental

Ni_2MnGa films with thicknesses (t) of 1, 3 and 4 μm with a Cr buffer layer were grown on (0 0 1) MgO substrates by DC magnetron sputtering. The target (diameter 3.8 cm and height 0.2 cm) was prepared using an induction furnace. The alloy with nominal composition Ni_2MnGa was previously encapsulated in a quartz tube under argon atmosphere. The films were grown in an atmosphere of 10 mTorr of argon with a power of 50 W. The substrate temperature for deposition was 623 K for the Cr buffer layer (thickness 120 nm) and 723 K for the Ni–Mn–Ga film. Lower deposition temperatures for the Ni–Mn–Ga films affect the crystalline structure increasing low-angle grain boundaries. The deposition rate was estimated from cross section scanning electron microscopy (SEM) images to be 33 (3) nm/min. After deposition, free-standing films were obtained by removing the thin chromium layer by wet-chemical etching using a conventional Cr etchant [9]. Only the free-standing 1-μm thin film could not be manipulated due to its buckling tendency. This work has been mainly focused on the 3-μm thin films.

The structure of the films was studied by transmission electron microscopy (TEM) with a Philips CM200UT microscope operating at 200 kV. TEM specimens were prepared using standard ion milling techniques in a Gatan PIP system. The composition was determined by energy-dispersive X-ray spectroscopy (EDS) in a Philips 515 SEM giving an accuracy of 0.5 at % using a Ni_2MnGa reference. The films were characterized by X-ray diffraction (XRD) in a Panalytical Empyrean equipment. The epitaxy of the film was confirmed using a four-circle diffractometer/goniometer.

Transformation temperatures such as M_s, martensite finish (M_f), austenite start (A_s) and austenite finish (A_f) were measured by electrical transport using conventional four-probe geometry in a vacuum cooling machine with a temperature rate (cooling down and warming up) of 1 K/min. The magnetization (M) measurements vs. temperature and magnetic field were performed using a commercial SQUID magnetometer. Out-plane dilation experiments in the 3-μm Ni–Mn–Ga film were performed by a capacitive technique. Magnetic fields up to 10 T were applied. The high resolution (0.1 nm) dilatometer [26] was placed in an evacuated environment with a low pressure ($p < 10^{-1}$ torr) of exchange ^4He gas. The roughness of the films was characterized using atomic force microscopy (AFM) with a Dimension 3100 Bruker equipment.

As we mention above, the free-standing 3-μm Ni_2MnGa film was encapsulated in a quartz tube under Ar atmosphere containing a small sample of the target alloy (≈1 gr). The role of this reference sample was to fix the Mn and Ga vapour pressure in order to avoid film degradation during the annealing at 1073 K [27].

3. Results and discussion

3.1. *As-grown films*

The epitaxial growth of a Ni–Mn–Ga film on (0 0 1) MgO has been confirmed by XRD analysis. As shown in Figure 1(a), in the XRD pattern of a supported 1-μm film, (0 0 1) peaks corresponding to the cubic austenitic ($L2_1$) Ni_2MnGa structure are observed, in

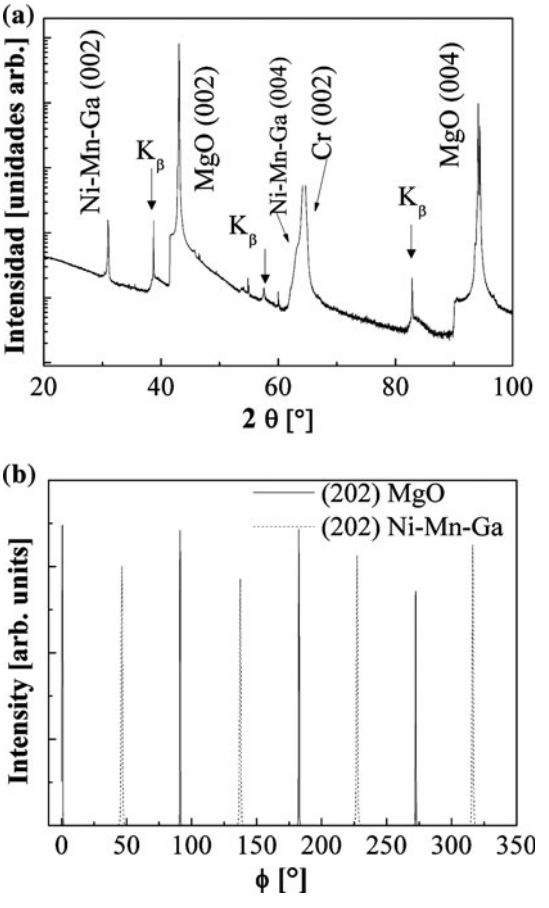

Figure 1. XRD patterns of a supported 1-μm $Ni_{47}Mn_{24}Ga_{29}$ film on (001) MgO. (a) θ–2θ scan. (b) Φ scans of the (2 0 2) Ni_2MnGa and (2 0 2) MgO. Reflections corresponding to the K_β spectral line are also included for the substrate and the film.

addition to the substrate (FCC MgO) and Cr buffer (BCC) layer reflections. The rocking curve FWHM of the (0 0 4) peak of the film was 0.54°. Also unidentified small reflections associated with the sampler holder appear at 2θ between 50 and 60°. The *a*- lattice parameter of the cubic austenitic structure is 0.577 nm, which is slightly smaller than that reported for the stoichiometric compound [28]. The epitaxial relationships between the film and the substrate are determined to be MgO(0 0 1)[1 0 0] ‖ Cr(0 0 1)[1 1 0] ‖ Ni–Mn–Ga(0 0 1)[1 1 0] (see Figure 1(b)) [9]. Similar XRD diffraction patterns were obtained in the other films (t = 3 and t = 4 μm). The root-mean-square (rms) surface roughness for a 4-μm film, measured by AFM from a 1 μm × 1 μm area, is 2 nm. EDS analysis shows that the film has a chemical composition of Ni 47 at %, Mn 24 at % and Ga 29 at % ($Ni_{47}Mn_{24}Ga_{29}$). This chemical composition indicates that the films are slightly rich in Ga and slightly poor in Ni and Mn (in comparison with target Ni_2MnGa). This chemical concentration corresponds to valence electron per atom (e/a) ≈ 7.3, and therefore, a smaller

M_s in comparison with the stoichiometric compound is expected [29]. On the other hand, 5M martensite is expected from the *e/a* ratio [19]. The presence of Cr was not detected at the bottom surface of free-standing films by EDS, which is consistent with previously published data in samples obtained using the same procedure [9]. Figure 2(a) shows a plan-view bright field TEM image of the 3-μm $Ni_{47}Mn_{24}Ga_{29}$ film. No grain boundaries were observed in a distance of 30 μm, which is consistent with the absence of high-angle grain boundaries due to the epitaxial growth observed in the Φ scans (Figure 1(b)). Only dislocations and some pores (diameter < 30 nm) appear. Similar pores have been observed by other authors at the surface of the films in SEM images [30]. The selected area electron diffraction (SAED) pattern shown in Figure 2(b) corresponds to the cubic austenitic ($L2_1$) structure in the [1 2 0] zone axis. No precipitates of secondary phases were observed in the TEM images.

The stoichiometric Ni_2MnGa undergoes a martensitic phase transition at $M_s \approx 200$ K [28]. Figure 3 shows the room temperature normalized resistance vs. temperature (*T*) for the three analyzed films supported on the substrates. The curves were rescaled for a clearer presentation. A shoulder close to 260 K is present in the three

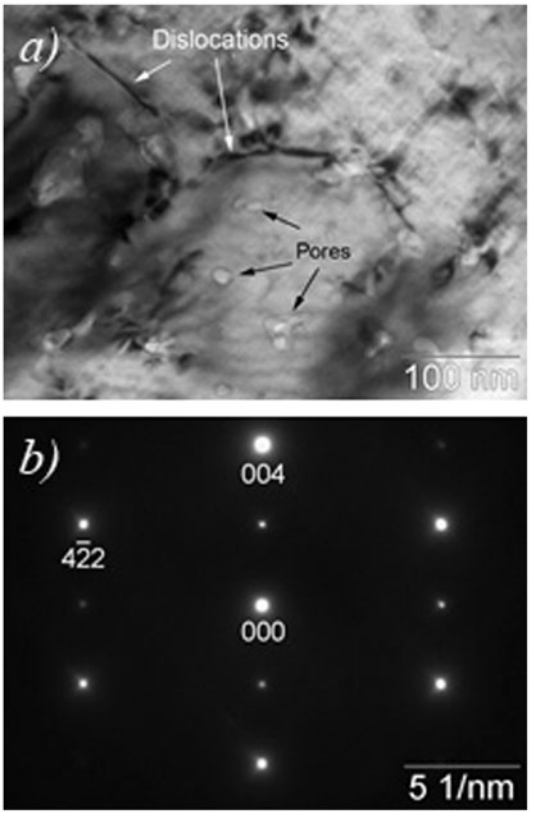

Figure 2. (a) Plan-view bright field TEM image of the 3-μm $Ni_{47}Mn_{24}Ga_{29}$ film. (b) SAED pattern corresponding to the cubic austenitic ($L2_1$) structure, zone axis [1 2 0].

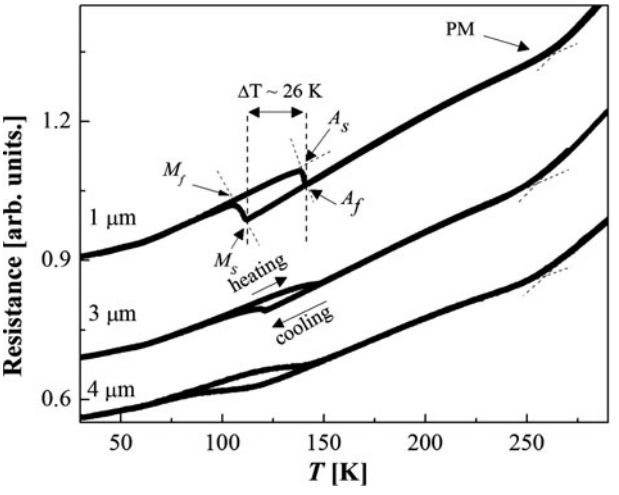

Figure 3. Electrical resistance vs. temperature (T) curves showing a pre-martensitic transformation (PM) and the martensitic transformation temperatures for the three studied film thicknesses. M_s: martensite start temperature. A_f: austenite finish temperature. ΔT: hysteresis of the martensitic transformation obtained as $A_f - M_s$. The resistance is normalized to room temperature and rescaled for a clearer presentation ($x1$, $x1.25$ and $x1.5$ for the 4-, 3- and 1-μm films, respectively).

samples and is associated with a pre-martensitic (PM) phase [28]. This PM phase is related to a modulation of the Ni, Mn and Ga sublattices, which renders a supercell with orthorhombic structure [31]. The summary of the transformation temperatures is presented in Table 1. When the films are cooled down, the martensitic transformation appears with $M_s \approx 120$ K, whereas in the warming up, full retransformation occurs at $A_f \approx 140$ K. The reduction in the M_s value of the films (in comparison with that expected for the target) is consistent with the changes in the chemical composition discussed above [17]. It is important to mention that although the M_s has a strong dependence with the chemical concentration, the three films have similar M_s values. However, a gradual increment in the extension of the transformation ($M_s - M_f$) is observed for thicker films, i.e. 7 K ($t = 1$μm), 17 K ($t = 3$ μm) and 25 K ($t = 4$ μm). This increment is opposite to that expected if internal strain induced by the interface with the substrate (huge for thin films) is considered, and it can be attributed to chemical gradients due to the high vapour pressure of Mn and Ga. In our case, chemical disorder is more important in thicker films since they spend a longer time at 723 K during the deposition. These gradients could modify locally the temperature for the

Table 1. Summary of the characteristic parameters of the martensitic transformation for as-grown supported $Ni_{47}Mn_{24}Ga_{29}$ films obtained from electrical transport.

Thickness (μm)	M_s (K)	M_f (K)	A_s (K)	A_f (K)	PM (K)
1	113 (2)	106 (2)	138 (2)	140 (2)	260 (3)
3	122 (2)	105 (3)	138 (3)	145 (2)	255 (3)
4	112 (2)	87 (3)	123 (3)	140 (2)	260 (3)

transformation. Post annealing process usually degrades the properties of Ni–Mn–Ga by evaporation of Mn and Ga, which reduce the M_s and increase the Curie temperature [32]. The hysteresis of the transformation defined as the difference between ($A_f - M_s$) is around 25 (3) K for different samples (Table 1). The hysteresis value can be related to the nature of the martensitic transformation and the microstructure of the films [14,33].

Magnetization measurements in films with $t = 3$ μm were taken as an overall characterization and a comparison between supported and free-standing films. From magnetization (M) vs. temperature (T) measurements, the Curie temperature of the austenite ($T_c = 392$ (3) K) and the martensitic transformation temperatures were obtained. Figure 4(a) shows a comparison of the martensitic transformation between a supported and a free-standing film (two different pieces of one film). The M_s values are within 5 K, which can be attributed to slight variations of composition for different pieces of the same film. In the supported film, the hysteresis is lower and the range of the transformation/retransformation is larger. This could be related to the strain at the interface in the supported film and to small changes in the topology of the films, due to the effects of the chemical etching during the separation of the substrate. It is known that small changes in the topology of the samples affect the mechanical behaviour of micrometric samples [34]. The strong change in the magnetization around the transformation is a sign of an expected change in the magnetocrystalline anisotropy of the samples. Figure 4(b) shows a comparison between the hysteresis loops obtained above (200 K) and below (70 K) the martensitic transformation in the supported film. The Ni_2MnGa has a saturation magnetization of ~2.4 μ_B/Mn [28]. In-plane hysteresis loops in the austenitic phase ($150\ K < T < T_c$) are close to being square, independently of the axis for the applied magnetic field (referred to the $[1\,0\,0]_A$ and $[1\,1\,0]_A$ identified by XRD). These loops are consistent with weak magnetocrystalline anisotropy [35,36]. In the martensitic phase, the hysteresis loops show a larger field for magnetic saturation (H_s), which is related to strong magnetocrystalline anisotropy. Below the M_s, hysteresis loops with **H** // surface along the initially identified $[1\,0\,0]_A$ and $[1\,1\,0]_A$ axis do not show features associated with twin motion [3]. The absence of magnetic field-induced strain was verified by measuring out of plane magnetostriction. The measurements were performed at $T < M_s$ and $\mu_0 H$ up to 10 T, after cooling down the sample from the austenitic phase without applied magnetic field. No appreciable magnetostriction (outside of the ordinary magnetostriction ≈0.03%) [37] and reversible magnetic hysteresis loops were observed. Absence of MSM effect is expected by considering the low M_s of the films [38]. Figure 4(c) shows the temperature dependence of the coercive field, with the magnetic field applied parallel to the surface along initially identified $[1\,0\,0]_A$ and $[1\,1\,0]_A$ axis. The large magnetocrystalline anisotropy in the martensite (≈1.63105 J/m^3 [6]) is manifested in a strong increment of the coercive field for both orientations at low temperatures. In addition, domain-wall pinning due to the polivariant microstructure can also contribute to the increment of the coercive field in the martensite.

3.2. *Annealed films*

As mentioned in the previous section, chemical inhomogeneities (chemical gradients), as well as internal strains, can be expected in the as-grown Ni–Mn–Ga films. It is know that sputtering produces spatial inhomogeneities. On the other hand, films obtained by sputtering usually present a chemical composition different to that expected for the

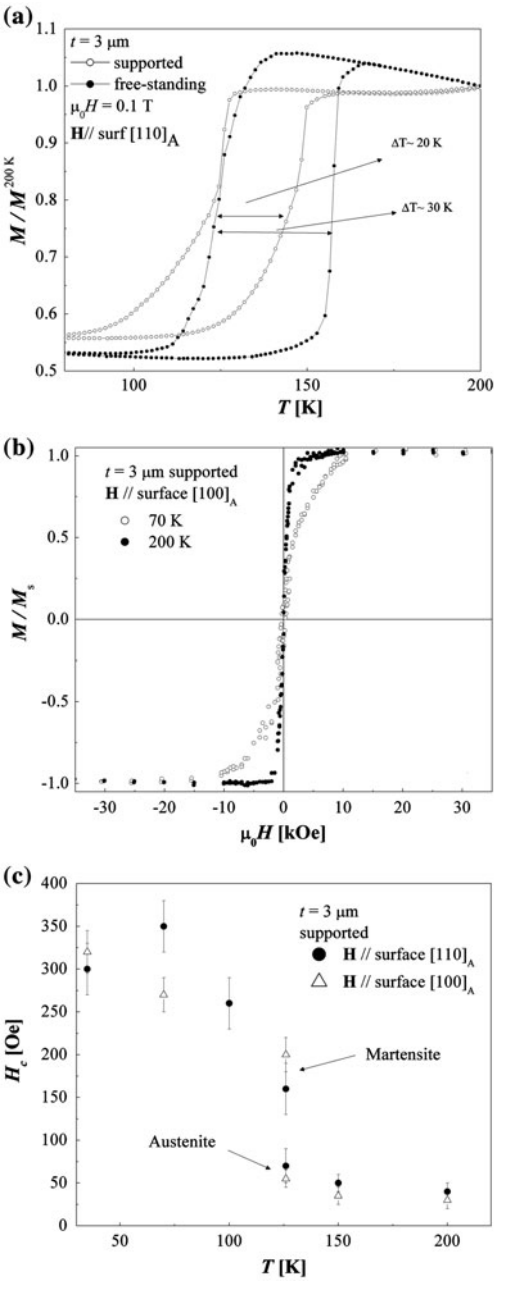

Figure 4. Martensitic transformations observed in a magnetization (M) vs. temperature (T) measurement corresponding to a supported and a free-standing 3-μm Ni–Mn–Ga film. The applied field with magnitude $\mu_0 H = 0.1$ T was parallel to the surface in the $[1\,1\,0]_A$ direction of the austenite. (b) Hysteresis loops obtained in the 3-μm supported film above (200 K) and below (70 K) the martensitic transformation. The applied field was parallel to the surface in the $[1\,0\,0]_A$ direction of the austenite. (c) Temperature dependence of the coercive filed with both **H** parallel to the surface ($[1\,1\,0]_A$ and $[1\,0\,0]_A$ directions) and **H** perpendicular to the surface of the supported films indicated in (a).

target [9]. The usual method to remove crystalline defects and inhomogeneities is thermal annealing. However, in Ni–Mn–Ga, the stoichiometry is affected by high vapour pressure of Ga and Mn [32]. In this way, by fixing the vapour pressure of the volatile elements with the presence of a bulk reference sample, thermal annealing provides homogenous samples [27]. Figure 5 shows a comparison of a 3-μm Ni–Mn–Ga film before and after annealing by 20 and 60 min at 1073 K. Noticeable differences appear in the film as a consequence of thermal annealing. First, the martensitic transformation temperature is increased by around 24 K (20 min) and 50 K (60 min), the latter being closer to the stoichiometric compound [28]. Second, the hysteresis of the transformation is strongly reduced from 30 to 17 K (20 min), and from 30 to 12 K (60 min). The chemical composition of the annealed film for 60 min corresponds to $Ni_{49}Mn_{26}Ga_{25}$ (obtained by EDS). Third, the extension of the transformation is gradually reduced. The T_c drops from 390 K ($Ni_{47}Mn_{24}Ga_{29}$) to 320 K ($Ni_{49}Mn_{26}Ga_{25}$). The difference in the hysteresis of the transformation can be associated with the intrinsic nature of the transformation and with the structure of remaining defects in the sample. The driving force ΔG generated by undercooling around the equilibrium thermodynamic temperature $T_0 = (M_s + A_f)/2$ can be related to the entropy change ΔS between the austenite and the martensite by $\partial\Delta G/\partial T = -\Delta S$. The ΔS value drops when the Ga content is increased [39], and the M_s systematically drops [14]. A narrower transition (for the same driving force) is expected for the annealed film by considering the change in chemical composition from $Ni_{47}Mn_{24}Ga_{29}$ ($\Delta S \approx 0.3$ J/mol K) to $Ni_{49}Mn_{26}Ga_{25}$ (0.5 J/mol K) [39]. On the other hand, the extension of the martensitic transformation ($M_s - M_f$) can be related to chemical gradients. They modify locally the M_s, producing wider transformations. The sharper transition for the annealed samples (see Figure 5) indicates that the chemical homogeneity is improved. The thermal annealing also should

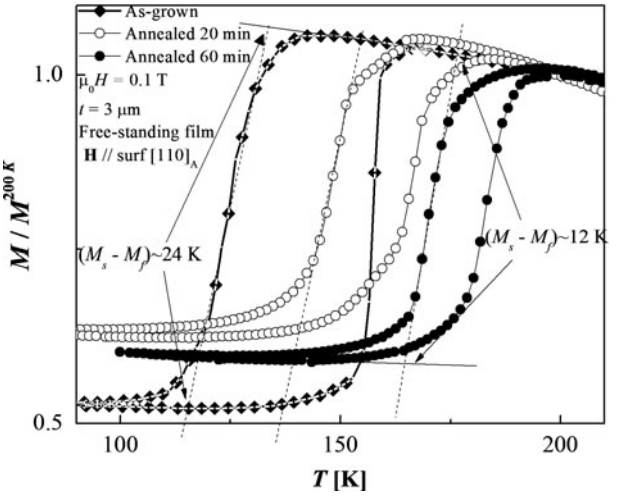

Figure 5. Normalized magnetization (M) vs. temperature (T) in the 3-μm film before ($Ni_{47}Mn_{24}Ga_{29}$) and after annealing for 20 and 60 min ($Ni_{49}Mn_{26}Ga_{25}$) at 1073 K. The applied field with magnitude $\mu_0 H = 0.1$ T was parallel to the surface in the $[1\,1\,0]_A$ direction of the austenite.

contribute to the removal of crystalline defects (such nanopores and dislocations). Magnetic measurements in the annealed films (below M_s) do not present features that can be associated with MSM (twin motion under applied magnetic field). The M_s value of the annealed films (close to the target composition) is in the limit for MSM [37]. MSM effect has been observed at ≈0.5 T in single crystals with low σ_{tw} [40].

In summary, we have grown epitaxial Ni–Mn–Ga thin films. We have observed that the chemical concentration of free-standing Ni–Mn–Ga thin films can be tuned by thermal annealing with a reference sample. In addition, sharper martensitic transformations are obtained. The removal of crystalline defects such dislocations, should contribute significantly to a reduction of the high σ_{tw} usually present in thin films grown by sputtering [9]. The strong influence of the chemical composition on the M_s [39] and the temperature dependence of σ_{tw} [37] indicate that thin films with martensitic transformation above room temperature are more promising for MSM. Futures studies should clarify the role of chemical inhomogeneities and crystalline defects on the σ_{tw}. The reduction of σ_{tw} in Ni–Mn–Ga thin films [9] to those observed in Ni–Mn–Ga single crystals [12,37,40] should contribute to enhance their performance for applications based in MSM devices.

4. Conclusions

Epitaxial Ni–Mn–Ga thin films have been grown using a target with nominal stoichiometric composition Ni_2MnGa. A shift to low temperatures in the M_s due to changes in the chemical composition in comparison with nominal composition of the target Ni_2MnGa, was observed. The martensitic transformation is weakly affected by the dimensionality in $Ni_{47}Mn_{24}Ga_{29}$ films with thickness between 1 and 4 μm. Thicker films present a gradual increment in the extension of the transformation, which indicates that chemical gradients are more relevant for longer time of deposition. A strong change in the magnetic anisotropy below the martensitic transformation is present in the films. However, no features associated with twin motion by an applied magnetic field have been observed. On the other hand, we have demonstrated that thermal annealing of free-standing thin films using a bulk reference allows tuning the M_s. In addition, a sharp martensitic transformation is observed for the annealed films. This can be associated with the reduction of chemical inhomogeneities and crystalline defects that locally modify the temperature for martensitic transformation. Due to the expected high sensitivity of σ_{tw} to the microstructure, thermal annealing helps to improve the properties of Ni–Mn–Ga thin films grown by sputtering. Further studies should be oriented to analyze the influence of chemical inhomogeneities and defects such as dislocations on σ_{tw}. For these studies, Ni–Mn–Ga thin films with more appropriate chemical composition (higher M_s) for MSM should be considered.

Acknowledgement

A.M.C, G.P.L., M.S., V.F.C and N.H. are members of CONICET (Argentina).

Disclosure statement

No potential conflict of interest was reported by the authors.

Funding

This work was supported by Consejo Nacional de Investigaciones Científicas y Técnicas of Argentina [CONICET PIP 11220090100457]; ANCYPT [PICT 2012-0884].

References

[1] E. Cesari, J. Pons, R. Santamarta, C. Segui and V.A. Chernenko, Arch. Metall. Mater. 49 (2004) p.791.
[2] V.A. Chernenko and S. Besseghini, Sens. Actuators, A 142 (2008) p.542.
[3] R. Kainuma, Y. Imano, W. Ito, Y. Sutou, H. Morito, S. Okamoto, O. Kitakami, K. Oikawa, A. Fujita, T. Kanomata and K. Ishida, Nat. Lett. 439 (2006) p.957.
[4] H.E. Karaca, I. Karaman, B. Basaran, Y.I. Chumlyakov and H.J. Maier, Acta Mater. 54 (2006) p.233.
[5] S. Kauffmann-Weiss, S. Hamann, M.E. Gruner, J.B. beck, A. Ludwig, L. Schultz and S. Fähler, Adv. Eng. Mater. 14 (2012) p.724.
[6] A. Sozinov, A. Likhachev, N. Lanska and K. Ullakko, Appl. Phys. Lett. 80 (2002) p.1746.
[7] A.M. Jakob, M. Hennes, M. Müller, D. Spemann and S.G. Mayr, Adv. Funct. Mater. 23 (2013) p.4694.
[8] O. Heczko, M. Thomas, J. Buschbeck, L. Schultz and S. Fähler, Appl. Phys. Lett. 92 (2008) p.072502.
[9] A. Backen, S.R. Yeduru, M. Kohl, S. Baunack, A. Diestel, B. Holzapfel, L. Schultz and S. Fähler, Acta Mater. 58 (2010) p.3415.
[10] J.W. Dong, J.Q. Xie, J. Lu, C. Adelmann, C.J. Palmstrøm and J. Cui, J. Appl. Phys. 95 (2004) p.2593.
[11] M. Ohtsuka, M. Matsumoto, K. Koike, T. Takagi and K. Itagaki, J. Magn. Magn. Mater. 310 (2007) p.2782.
[12] S.J. Murray, M. Marioni, S.M. Allen, R.C. O'Handley and T.A. Lograsso, Appl. Phys. Lett. 77 (2000) p.886.
[13] B. Yang, Z.B. Li, Y.D. Zhang, G.W. Qin, C. Esling, O. Perroud, X. Zhao and L. Zuo, Acta Mater. 61 (2013) p.6809.
[14] X. Xu, M. Nagasako, W. Ito, R.Y. Umetsu, T. Kanomata and R. Kainuma, Acta Mater. 61 (2013) p.6712.
[15] C. Seguí, V.A. Chernenko, J. Pons, E. Cesari, V. Khovailo and T. Takagi, Acta Mater. 53 (2005) p.111.
[16] J. Pons, R. Santamarta, V.A. Chernenko, E. Cesari, Mat. Sci. Eng. A 438–440 (2006) p.931.
[17] N. Lanska, O. Söderberg, A. Sozinov, Y. Ge, K. Ullakko and V.K. Lindroos, J. Appl. Phys. 95 (2004) p.8074.
[18] G. Jakob, T. Eichhorn, M. Kallmayer and H. Elmers, Phys. Rev. B 76 (2007) p.174407.
[19] K. Tsuchiya, H. Nakamura, D. Ohtoyo, H. Nakayama, H. Ohtsuka and M. Umemoto, Int. J. Mater. Prod. Tec. Special Issue, SPM1 (2001) p.409.
[20] S. Kaufmann, R. Niemann, T. Thersleff, U.K. Rößler, O. Heczko, J. Buschbeck, B. Holzapfel, L. Schultz and S. Fähler, New J. Phys. 13 (2011) p.053029.
[21] P. Müllner, V.A. Chernenko and G. Kostorz, Scr. Mater. 49 (2003) p.129–133.
[22] O. Söderberg, A. Sozinov, Y. Ge, S.–P. Hannula and V.K. Lindroos, Giant Magnetostrictive Materials, in *Handbook of Magnetic Materials*, K.H.J. Buschow, ed. Vol.16, Elsevier Science, Amsterdam, 2006.
[23] A.A. Likhachev and K. Ullakko, Phys. Lett. A 275 (2000) p.142.
[24] J. Enkovaara, A. Ayuela, L. Nordström and R.M. Nieminen, Phys. Rev. B 65 (2002) p.134422.

[25] N. Lanska, O. Soderberg, A. Sozinov, Y. Ge, K. Ullakko and V.K. Lindroos, J. Appl. Phys. 95 (2004) p.8074.
[26] G.M. Schmiedeshoff, A. W. Lounsbury, D. J. Luna, S. J. Tracy, A. J. Schramm, S. W. Tozer, V. F. Correa, S. T. Hannahs, T. P. Murphy, E. C. Palm, A. H. Lacerda, S. L. Bud'ko, P. C. Canfield, J. L. Smith, J. C. Lashley and J. C.Cooley, Rev. Sci. Instrum. 77 (2006) p.123907.
[27] N. Haberkorn, M. Ahlers and F.C. Lovey, Scr. Mater. 61 (2009) p.821.
[28] P.J. Brown, J. Crangle, T. Kanomata, M. Matsumoto, K.-U. Neumann, B. Ouladdiaf and K.R.A. Ziebeck, J. Phys.: Condens. Matter 14 (2002) p.10159.
[29] V.A. Chernenko, Scr. Mater. 40 (1999) p.523.
[30] S.R. Yeduru, A. Backen, C. Kübel, D. Wang, T. Scherer, S. Fähler, L. Schultz and M. Kohl, Scr. Mater. 66 (2012) p.566.
[31] A. Planes, L. Mañosa, A. Saxena (Eds.), *Magnetism and Structure in Functional Materials*. Springer Series in Materials Science, Springer, Vol. 79, 2005.
[32] A. Backen, R. Niemann, S. Kaufmann, J. Buschbeck, L. Schultz and S. Fähler, ESOMAT 2009 – Proceeding of 8th European Symposium on Martensitic Transformations, in Proceedings (2009) p.4002.
[33] N. Haberkorn, A.M. Condó, C. Espinoza, S. Jaureguizahar. J. Guimpel and F.C. Lovey, J. Alloys Compd. 591 (2014) p.263.
[34] S.M. Ueland and C.A. Schuh, Acta Mater. 61 (2013) p.5618.
[35] Q. Pan, J.W. Dong, C.J. Palmstrøm, J. Cui and R.D. James, J. Appl. Phys. 91 (2002) p.7812.
[36] R. Tickle, R.D. James, T. Shield, M. Wuttig and V.V. Kokorin, IEEE Trans. Magn. 35 (1999) p.4301.
[37] O. Heczko, J. Magn. Magn. Mater. 290–291 (2005) p.846.
[38] O. Heczko and L. Straka, J. Appl. Phys. 94 (2003) p.7139.
[39] X. Xu, T. Kanomata and R. Kainuma, Acta Mater. 79 (2014) p.159.
[40] O. Heczko, A. Sozinov and K. Ullakko, IEEE Trans. Magn. 36 (2000) p.3266.